Geotech Geol Eng (2022) 40:3393–3412
https://doi.org/10.1007/s10706-022-02100-1

ORIGINAL PAPER

Evaluation of the Group Effect's Simulation on the Bearing Capacity of Bored Piles in Granular Soil, Using Load Transfer Functions

Edno Cerqueira Junior · Alfran Sampaio Moura

Received: 27 May 2020 / Accepted: 1 March 2022 / Published online: 10 March 2022

Abstract Load transfer functions, such as the t-z and q-z curves, combined with numerical methods implemented by computational programs are nowadays widely used in geotechnical design of deep foundations. It is known that in this type of design, piles are more often employed in groups instead of isolated. Within this context, the purpose of this research was to estimate the bearing capacity of groups of bored piles, installed in granular soil, using t-z and q-z curves suggested by Reese and O'Neill (1988). The geotechnical design program RS Pile was used in the simulation of an isolated pile's load–displacement curve. The result was used along with group settlement factors (ξ) in order to predict the load-displacements curves of several pile groups, the graphics obtained were used to estimate the bearing capacities of the groups. Lastly, all the predictions were compared with experimental data obtained from load tests carried out in foundations installed in the Experimental Field of Geotechnics and Foundations of the Federal University of Ceará (CEGEF-UFC). For the isolated piles, the difference between the simulated and experimental values of bearing capacities ranged from -11% to 5% and the settlement predictions were also accurate. For the pile groups, regarding the settlement prediction, the compared curves showed agreement for the design load for 6 out of the 7 groups analyzed. Regarding the bearing capacity, the difference between the predicted to the experimental values ranged from -8% to 20%. Thus, the employed method was able to produce accurate predictions.

Keywords Load transfer functions · Numerical analysis · Prediction of settlements · Prediction of bearing capacities · Piled rafts

1 Introduction

Among the several types of foundation employed in civil construction, piles are a very common one. This type of deep foundation is actually more often used in groups, instead as an isolated element. Axially loaded piles are very frequently analyzed through the t-z method. In the mentioned methodology the piles are broken into a series of segments, being each one supported by a spring. The piles are then represented by a discrete nonlinear system of springs to take into account side friction (t-z springs) and end bearing (q-z springs) resistances.

Several studies have been conducted regarding load-transfer functions such as the t-z and q-z curves. Nanda and Patra (2014) proposed a method to predict t-z and load-settlement curves, accounting for the nonlinear stress–strain, hardening and softening

E. C. Junior (✉) · A. S. Moura
Department of Hydraulic and Environmental Engineering, Federal University of Ceará, Fortaleza, Ceará, Brazil
e-mail: ednocjr@gmail.com

A. S. Moura
e-mail: alfransampaio@ufc.br

response of soil-pile interaction, and using laboratory tests for the prediction of soil's behavior in field conditions. It was found in the outcomes of the referred research good agreement between predicted values and experimental data, as well as that the suggested methodology can be applied to pile groups.

Zhang et al. (2018) mention a list of models used to apply the load-transfer curves method, among which are the softening and the hyperbolic models. The first one is used in the paper to relate skin friction with pile-soil relative displacements, while the second one is used similarly for the pile's end. The study indicates good agreement between the employed method and experimental data, besides showing that the methodology applied was capable of assessing the failure features of skin friction.

Zhu and Chang (2002) presented an approach to evaluate load-transfer curves for bored piles embedded in residual soil and in weathered rocks by the consideration of modulus degradation, experimental data from different locations were used in the verifications of the adopted procedure. In the cited paper, it was concluded that the t-z and subsequently load-settlement curves could be accurately predicted by the technique employed.

Concerning the group effect in piles, Sharafkhah and Shooshpasha (2018) performed experiments with cast-in-place bored concrete piles and reinforced concrete raft including: single pile; single pile in a goup; unpiled raft; free-standing pile group with 4 or 9 piles; and piled rafts with 4 or 9 piles. The research aimed mainly to compare the performances of piled rafts foundations with free-standing pile groups in sand. The concluding remarks were: a single pile installed in a group has its bearing capacity and stiffness increased, this effect is larger in the internal elements of the group; piles installed beneath a cap have their bearing capacity increased, while the capacities of the caps are reduced, it's observed the effects are mutually neutralized.

Garcia and Albuquerque (2018) investigated the influence of relative stiffness on the behavior of piled raft by analyzing several configurations of this type of foundation with different number of piles and raft's thickness. The authors found that, on average, 80% of the load supported by the piles was absorbed by the shaft's elements and 20% by their ends. It was also concluded in the research that the contribution of the piles to the foundations analyzed varies with their position and with the piled raft's thickness, among other concluding remarks.

Cunha and Poulos (2018) investigated the importance of the excavation level in the settlement's prediction of piled rafts. A case reported in the literature of a house founded over a soft highly plastic marine clay in Gothenburg, Sweden, was used in the analysis. The study showed the relevance in design of the understanding of the input parameters such as: raft's geometry; load distribution; level and sequence of the excavation; variability of the water level; soil strata; and test´s programs both in laboratory and in field.

This paper presents an evaluation of the group effect of piles bored in granular soil based on a simulation using t-z and q-z curves combined with the finite element method (FEM), implemented by RS Pile. Based on load tests carried out in single piles in the Experimental Field of Geotechnics and Foundations of the Federal University of Ceará (CEGEF-UFC), the load–displacement curve of a single pile was simulated in the cited program. Applying group settlements factors (ξ) in the obtained curve, load–displacement curves of the pile groups of the referred experimental field were simulated. Using the pile group's curves, the bearing capacities of these groups were estimated and the results were compared with experimental values obtained from load-tests performed in the pile groups.

2 Material and Methods

- This research was developed according to the following sequence:
- Definition of the location of the study;
- Geotechnical characterization of the studied soil profile;
- Definition of the input parameters and model simulated;
- Simulations of the load–displacement curves of the piles and prediction of the pile group's bearing capacities;
- Comparisons of the predicted values with the experimental data obtained from load tests.

The research was developed with data collected from the CEGEF-UFC, in Fortaleza, Ceará-Brazil, an image and the location of the experimental field are presented in Fig. 1. Figure 2 shows an image and a

schematic plan of the foundations installed in the CEGEF-UFC, it can be seen that there are 26 piles distributed under 10 caps. All the piles are 1.5 m in length and 0.1 m in diameter. The pile groups are composed of 2 and 4 elements, with different distances between the piles. A summary of the information about the foundations analyzed in this study is presented in Table 1, the dimensions presented in the table are illustrated in Figs. 2 and 3. The caps in the cited Table can be observed in the mentioned plan. The relative spacing (s/D), also in Table 1, corresponds to the distance between the piles in caps, expressed in number of diameters.

Despite the reduced dimensions of the foundations analyzed in this research, Nasr (2014) stated that the factors that must be considered in the usage of small-scale models are the soil particle size, construction techniques and boundary conditions. Considering that according to Franke and Muth (1985), scale error is not relevant for a ratio of the pile diameter to the mean grain size (D_{50}) greater than 30 and that is the case of this study, the particle size condition is fulfilled. Concerning the two other mentioned factors,

Fig. 1 Experimental Field of Geotechnics and Foundations of the Federal University of Ceará (Google Maps 2019).

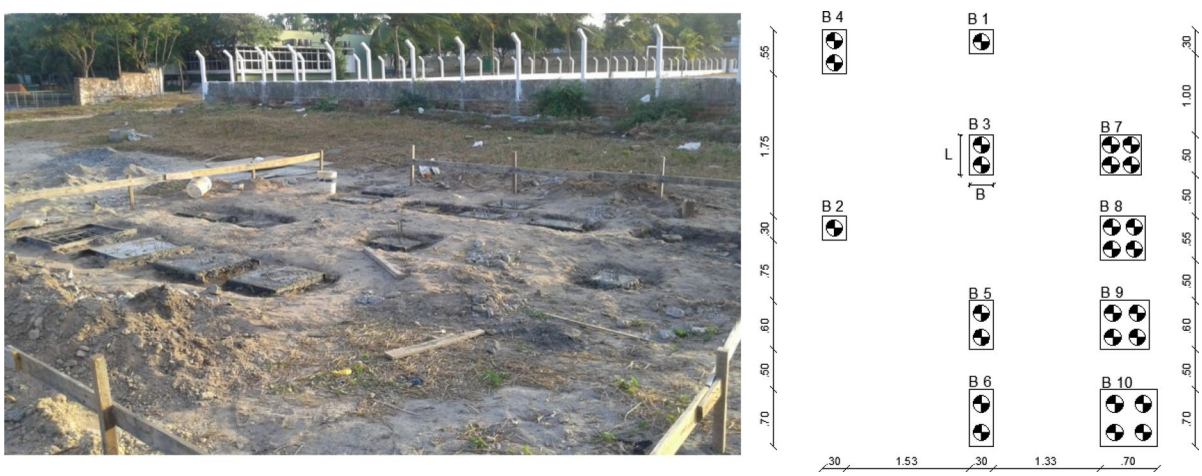

Fig. 2 **a** Photo and **b** schematic plan of the foundations analyzed (adapted from Cerqueira Junior 2019)

Table 1 Summary of the information about the piles

Cap n°	s/D	N° of piles	Cap			L_P (cm)
			L (cm)	B (cm)	H (cm)	
1	–	1	30	30	20	150
2	–	1	30	30	20	150
3	2	2	50	30	20	150
4	2,5	2	55	30	25	150
5	3	2	60	30	30	150
6	4	2	70	30	35	150
7	2	4	60	60	30	150
8	2,5	4	65	65	35	150
9	3	4	70	70	40	150
10	4	4	80	80	50	150

The ratio s/D refers to the distance between the piles' axes, s, and diameters, D (10 cm), which are the same for all piles

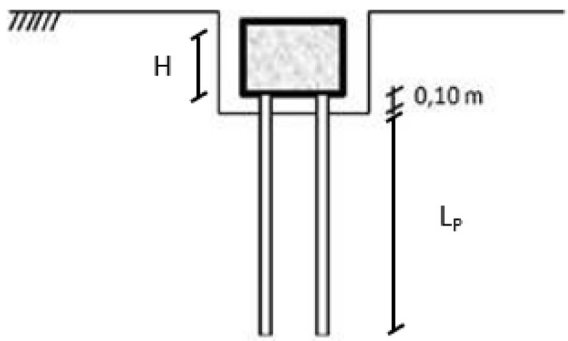

Fig. 3 Illustration of 2 pile group in CEGEF-UFC (Bonan et al. 2020)

the tests showed in this paper are supposed to represent the behavior of full-scale bored piles installed in a similar soil profile as the reduced models. Thus, the small-scale tests performed in this research tend to be representative of large-scale foundations.

In order to determine the properties of the soil profile analyzed in this research, both laboratory and field tests were performed. The laboratory tests included: sieve analysis; bulk density; Atterberg limits; moisture content. The conventional field test carried out was a Standard Penetration Test (SPT). The laboratory tests were performed with soil samples from three depths: 0.20 m; 0.60 m; and 1.10 m. The Atterberg tests indicated cohesionless soil for all the samples. The sieve analysis demonstrated the soil to be sandy, predominantly homogenous, with nearly 10% of clay and silt. The particle size distribution curves are shown in Fig. 4.

For the sample from the most superficial depth (20 cm), the percentages of material are: 87% of sand; 4% of silt; and 9% of clay. For the sample from the intermediate depth (60 cm), the percentages are the following: 86.5% of sand; 1.5% of silt; and 12% of clay. At last, for the sample from 110 cm depth, the quantities are: 83% of sand; 4% of silt; and 13% of clay. The bulk density was determined by the usage of the picnometer. For the calculus of the moisture content, it was used the drying oven. A summary of laboratory tests' results is presented in Table 2.

Regarding the in situ tests, the Standard Penetration Test (SPT) report is shown in Fig. 5. As it can be observed, the standard penetration resistance (N-value) ranges from 12 to 18 until 4 m depth. Below the mentioned depth the N-value decreases rapidly reaching 5.7 at 5 m depth and 3.5 at 7 m depth. The ground water level (G.W.L.) was determined at 7.35 m depth. Load tests were carried out on all the piles installed in the CEGEF-UFC. The procedures of the tests carried out in the experimental field is illustrated in the Figs. 6 and 7.

Initially, it was simulated the behavior of a single pile, which the features were previously presented and can be observed in Table 1. The characteristics of the soil profile in which the single pile simulated was installed were also commented. For the simulation, it was used the RS Pile, it applies load transfer functions, such as t-z and q-z curves, combined with the FEM in the prediction of deep foundation's settlements. The program uses the mentioned model of a discrete nonlinear system of springs to represent the lateral and end's resistances of piles, the applied method is presented in this section.

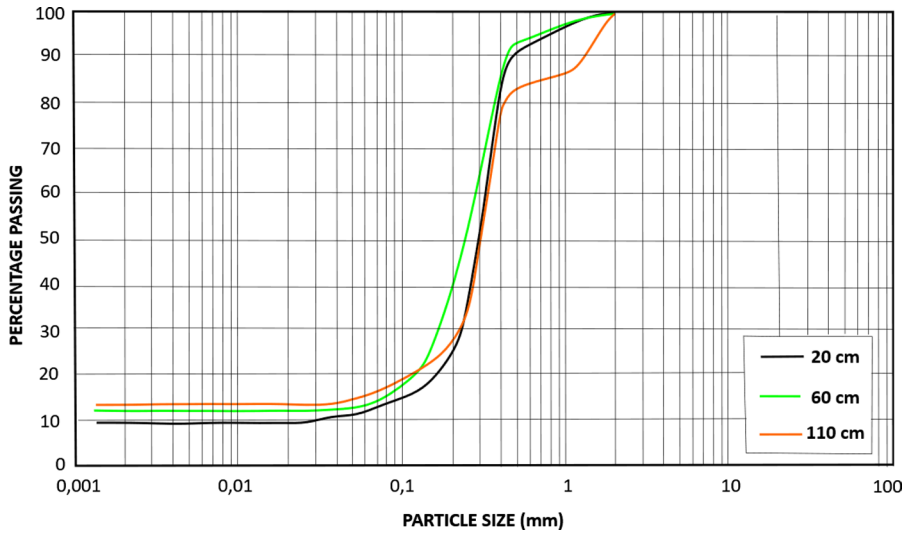

Fig. 4 Particle size distribution curve (Moura et al. 2018)

Table 2 Summary of the results of the laboratory tests (adapted from Moura et al. 2018)

Characteristics/ parameters	20 cm	60 cm	110 cm	Procedure
Soil classification (USCS)	SM	SM	SM	Sieve analysis
Moisture content (%)	4,9	11,13	12,4	Stove
G_s (g/cm^3)	2,51	2,54	2,58	Picnometer

In order to perform the simulations, it was first necessary to define a t-z and a q-z curve. RS Pile offers 3 options of curves for granular soils: API Sand (American Petroleum Institute); Mosher Sand; and Drilled Sand. Each option is based on different proposals presented in the literature. Besides the cited curves, the program also allows the user to manually insert some other load transfer function. The first option was developed for driven piles. The second was a proposal elaborated by Mosher (1984) based on experimental tests and on the literature. The last curve uses functions suggested by Reese and O'Neill (1988), which were generated specifically for bored piles.

The API curve was not selected for the present research due to be proper for piles installed by a method different than the used in the foundations analyzed in this case. The Mosher option was also not chosen for not being specific for the type of piles used in this study. Therefore, the Drilled Sand functions were defined to be implemented in the simulation. It is worth mentioning that the results obtained using the selected option showed better agreement with the experimental data than the ones obtained through the usage of the other curves.

The Drilled Sand functions are, as mentioned, the t-z and q-z curves proposed by Reese and O'Neill (1988), the graphics are presented in Figs. 8 and 9. The curves associate, for the shaft and the tip of the pile, the load transfer, normalized by the load capacity, to the displacements, normalized by the shaft's diameter. The presented functions incorporate the non-linear stress–strain behavior of the soil. The methodology implemented by the adopted program uses a system of springs to represent an axially loaded pile, illustrated in Fig. 10. The springs in the mentioned figure represent the structural element and the soil's mechanisms of resistance: soil friction and end bearing.

In order to obtain the displacement and load transfer profiles of the pile for a single value of load applied on its top, the structure is divided in segments. The calculus made by the program is based on a force equilibrium of an infinitesimal segment, presented in Fig. 11, from which a governing differential equation (Eq. 1) is deducted. The settlements are then calculated by computing the stiffness of each segment in several iterations, using the FEM. The stiffness of each element of the pile is obtained through its geometry and Young's Modulus, data given in this section. The stiffness of each soil element of the shaft is calculated

DEPTH (m)	BLOW COUNT – 15 cm			N_{SPT}	BLOW COUNT – 30 cm 2ª + 3ª (10 20 30)	DEPTH (m)	DESCRIPTION
	1ª	2ª	3ª			0,00	
0,20 0,65	4	8	7	15			Fine silty sand, grey, medium compactness
1,00 1,45	5	5	7	12		1,4	
2,00 2,45	6	8	7	15			Sandy silt, yellow, medium compactness
3,00 3,45	7	9	9	18		3,00	
4,00 4,45	7	9	9	18			Sandy silt, yellow with red pigmentation, low to medium compactness
5,00 5,45	2	3	2,7	5,7		6,00	
6,00 6,45	1	1,9	1,5	3,4		GWL 7.35m	Sandy silt, parti-colored, loose
7,00 7,45	1,9	1,8	1,7	3,5		7,51	

Fig. 5 Standard Penetration Test report (Moura et al. 2018)

Fig. 6 Load test being carried out in CEGEF-UFC (Bonan et al., 2020)

using the t-z curve. The end bearing resistance is obtained through the cross-sectional area of the pile and the unit end bearing resistance given in force per area.

Fig. 7 Load being applied on a cap in CEGEF-UFC (Bonan 2017)

$$-EA\frac{d^2u_z}{dz^2} = \tau C \quad (1)$$

where E = pile segment modulus of elasticity at depth z, A = pile segment cross sectional area at depth z, u_z = pile segment displacement at depth z due to applied loads, τ = soil unit skin friction at depth z, C = circumference of pile segment at depth z.

For the simulation conducted in this research, the program was set to divide the pile in 50 segments and perform 100 iterations with a convergence tolerance of 0,0001. Each segment is composed of two elements of pile and, in between them, one element of soil. The assumptions of the method to apply the FEM are: pile is geometrically straight and second order effects are neglected; eccentric loads are neglected; pile keeps its initial geometry; material is isotropic.

To proceed the simulation, it was necessary to define bearing capacities for the shaft and end of the pile. Among several semi-empirical methods used, Teixeira (1996) showed the best agreement with the values determined from load-tests. According to Cintra and Aoki (2010), the mentioned method is widely used in geotechnical design in Brazil, besides being also employed abroad, it is based on a correlation with SPT, corrected by load tests, Eq. 2 presents the expression for Teixeira (1996). The input parameters of the cited equation are shown

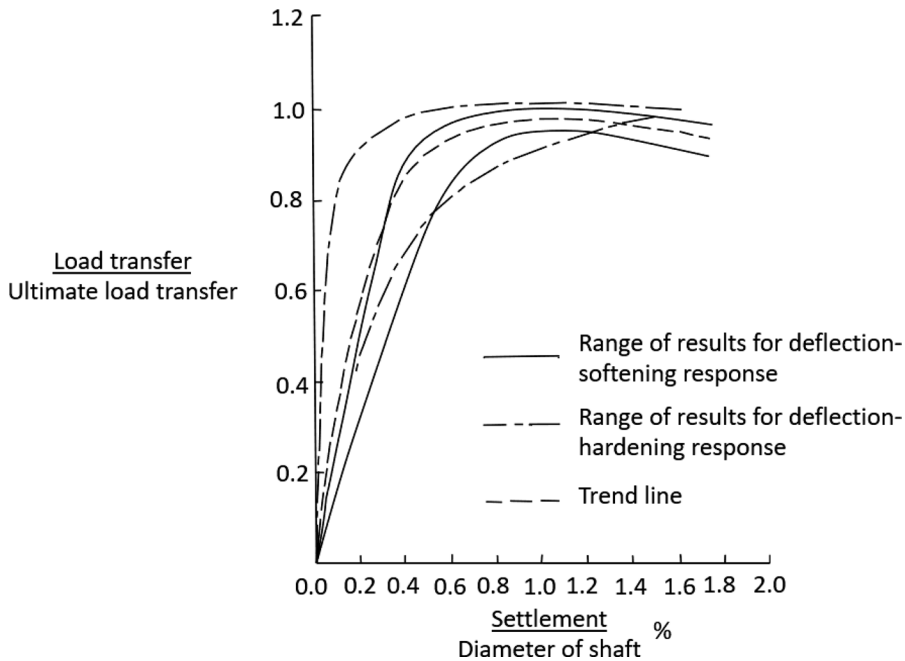

Fig. 8 Skin friction (t-z) curve (adapted from Reese and O'Neill 1988)

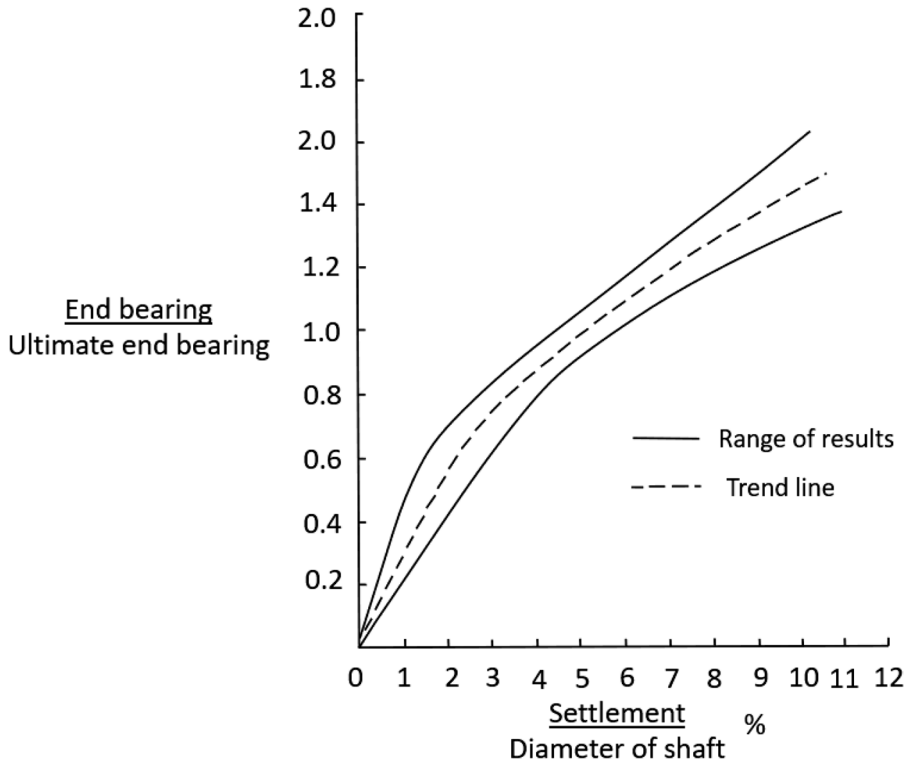

Fig. 9 End bearing (q-z) curve (adapted from Reese and O'Neill 1988)

in Tables 3 and 4. The resistances for the shaft and end of the pile inserted in the program, obtained through the mentioned method, were 32.8 kN and 30.8 kN, respectively. As the program requires the resistances in terms of stresses, the cited values were then divided by the corresponding lateral and end's area.

$$Q_u = Q_T + Q_S = \alpha N_P A_P + \beta N_L UL \quad (2)$$

where Qu = Ultimate bearing capacity of the pile foundation, Q_T = Tip capacity, Q_S = Shaft's capacity, α = Tip resistance's parameter depending on the types of soil and pile, β = Shaft resistance's parameter depending on the type of pile, N_P = Average N_{SPT} within the length of 4 diameters above the tip and 1 diameter below it, N_L = Average N_{SPT} within the length of the shaft, A_P = Area of the tip, U = Perimeter of the shaft, L = Axial length of the pile.

The geometric characteristics of the piles are summarized in the Table 1. In addition to the information presented in the cited table, it is worth to comment that the piles are perpendicular to the soil's surface, which is flat. The stress–strain response of the piles (structural element) was considered elastic and its Young's modulus equal to 30.1 GPa, this value was determined in simple compression tests.

The model simulated in the program of the single pile embedded in the subsoil is shown in Fig. 12. As it can be seen, the pile is not connected with a cap, that's because, in the program used, caps are only for the case of pile groups. It is important to outline then that the foundations analyzed in this study were installed in the CEGEF-UFC without ground contact, therefore, with the piles resisting only through their shafts and ends, thus the simulation represents this field condition.

For the prediction of the load–displacement curve of the single pile, each load stage of the load tests was simulated. The outcomes of each simulation were the displacements along the pile and also the load transfer diagram. The load–displacement curve was generated from the settlements predicted for the top of the pile of all load stages.

The load–displacement curves of the pile groups were generated from the simulated single pile's curve. First, it was necessary define a method to the determine

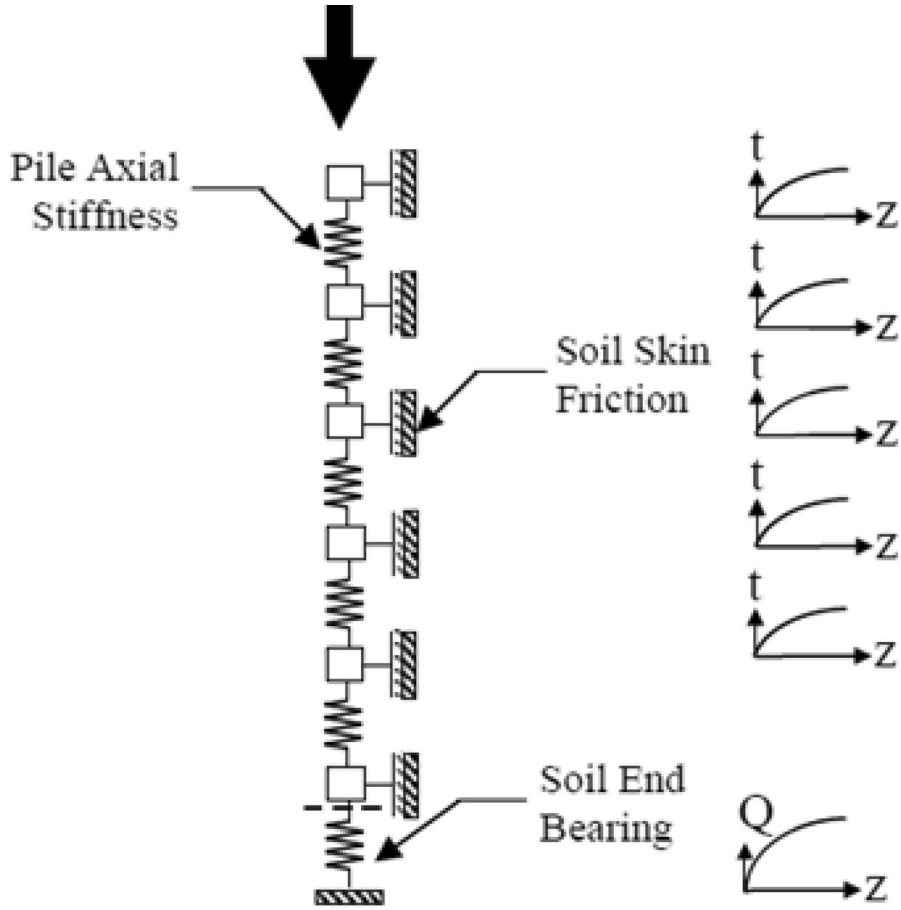

Fig. 10 Spring-mass model for the pile embedded in soil (Rocscience 2018)

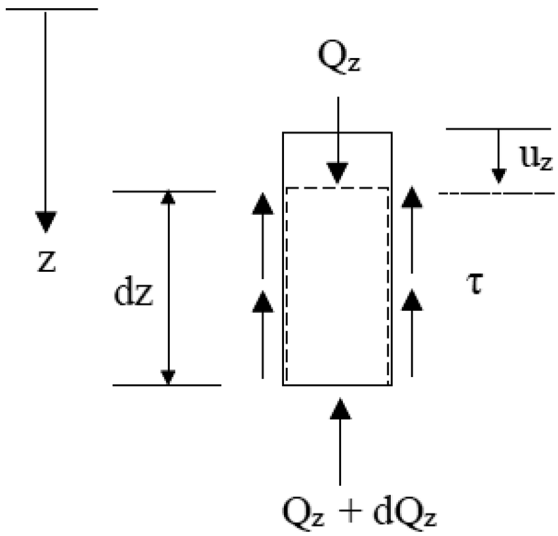

Fig. 11 Free body diagram of a pile segment (Rocscience 2018)

Table 3 Values for the parameter α (Teixeira 1996)

Soil ($4 < N_{SPT} < 40$)	Type of pile—α (kPa)			
	Precast steel pile	Franki pile	Open pit bored pile	Root pile
Silty clay	110	100	100	100
Clayey silt	160	120	110	110
Sandy clay	210	160	130	140
Sandy silt	260	210	160	160
Clayey sand	300	240	200	190
Silty sand	360	300	240	220
Sand	400	340	270	260
Gravelly sand	440	380	310	290

the settlement factor (ξ), which is the ratio of the settlement of a group of piles to the settlement of a single pile with the same characteristics and under the same load per pile, according to Eq. 3. In order to define

Table 4 Values for the parameter β (Teixeira 1996)

Type of pile	β (kPa)
Precast steel pile	4
Franki pile	5
Open pit bored pile	4
Root pile	6

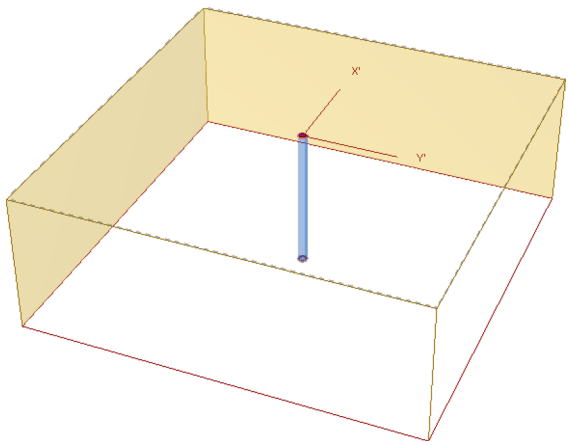

Fig. 12 Single pile's model simulated

the method, both experimental results and empirical expressions were used. The empirical formulas for the settlement factor (ξ) proposed by Skempton (1953), Vesic (1969) and Fleming et al. (1985) were applied to estimate the factors for all the pile groups, the expressions are presented in Eqs. 4, 5 and 6, respectively. The settlement factors (ξ) were also obtained experimentally by dividing, for the same load per pile, the settlement measured in the load tests of each group by the one measured for the single pile (cap 2). All the settlement factors (ξ) obtained are presented in the Tables 5 and 6.

$$\xi = \frac{w_g}{w_s} \tag{3}$$

$$\xi = \left(\frac{4B_g + 3}{B_g + 4}\right)^2 \tag{4}$$

$$\xi = \sqrt{\frac{B_g}{D}} \tag{5}$$

$$\xi = n^y \tag{6}$$

where w_g = Settlement of a pile group for a specific value of load per pile, w_s = Settlement of a single

Table 5 Settlement factors (ξ), experimental and estimated, for the 2 piles' groups

Caps	Settlement for 34.3 kN per pile	Experimental	Skempton (1953)	Vesic (1969)	Fleming et al. (1985)
2	0.59	–	–	–	–
3	0.70	1.19	0.96	1.67	1.26
4	0.37	0.63	1.00	1.81	1.26
5	1.25	2.12	1.03	1.94	1.26
6	1.98	3.36	1.10	2.18	1.26

Table 6 Settlement factors (ξ), experimental and estimated, for the 4 piles' groups

Caps	Settlement for 17.2 kN per pile	Experimental	Skempton (1953)	Vesic (1969)	Fleming et al. (1985)
2	0.22	–	–	–	–
7	0.34	1.55	1.03	1.96	1.58
8	3.39	1.41	1.08	2.13	1.58
9	0.47	2.14	1.13	2.29	1.58

pile for a specific value of load per pile, B_g = width of group pile section, D = width or diameter of each pile in the group, n = number of piles of the group, y = exponent that ranges from 0.4 to 0.6 for most groups, Poulos (1989) *apud* Velloso and Lopes (2010) suggests 0.33 for floating piles in sand and 0.5 for piles in clay.

The data presented in the Tables 5 and 6 were analyzed and, considering the experimental factors as reference, the method of Vesic (1969) was selected to be employed in this research. The results obtained through the mentioned method showed best agreement with the experimental values for the caps 5, 6, 8 and 9. For the cap 7, Vesic (1969) led to better results than Skempton (1953). Once the method for the settlement factors (ξ) was selected, the load–displacement curves of the pile groups were generated. As previously mentioned, the pile group's curves were obtained from the simulated single pile load displacement curve. For each group, the loads of the single pile's graphic were multiplied by the corresponding number of piles of the group and the displacements of single pile were multiplied by the corresponding settlement factor (ξ).

The simulated load–displacement curves were plotted along with the experimental curves of the pile groups, obtained from load tests. The predicted and the experimental settlements were compared, special attention was given to the displacements at the design load. The bearing capacities of the pile groups were calculated from both the simulated and the experimental load-displacements curves through two methods, Van der Veen (1953) and one provided by the Brazilian technical rule NBR 6122 (ABNT 2019), the results obtained were compared.

The mentioned methods obtain the bearing capacity of a pile foundation based on different criteria. Van der Veen (1953) extrapolates a load–displacement curve to find the load for which the graphic is supposed to tend asymptotically, predicting a physical failure. In order for the described method to be applied, an arbitrary value of bearing capacity must be used to plot points with the coordinates given by Eq. 7 and the corresponding loads. The points obtained with the arbitered bearing capacity must form a line with the r-squared as high as possible, the value for which it happens is considered the bearing capacity, Fig. 13 illustrates the described procedure.

$$w = -\ln\left(1 - \frac{Q}{Q_u}\right) \tag{7}$$

w = settlement of the pile, Q = Loads from the load–displacement curve, Qu = Bearing capacity arbitrated.

The Brazilian technical rule NBR 6122 (ABNT 2019) provides a method based on a linear equation (Eq. 8) in slope-intercept form, given by the sum of an elastic compression of the structural element with a fraction of the shaft's diameter. The linear equation must be plotted along with the load–displacement curve of the pile and the bearing capacity is the load corresponding to the intercept point of both graphics, Fig. 14 illustrates the described procedure.

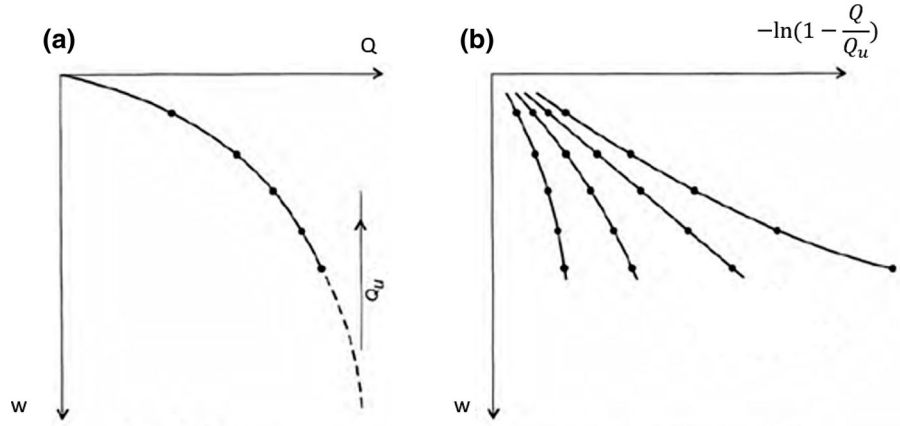

Fig. 13 **a** Extrapolation of a load–displacement curve by the (**b**) Van der Veen (1953) method (adapted from Velloso and Lopes 2010).

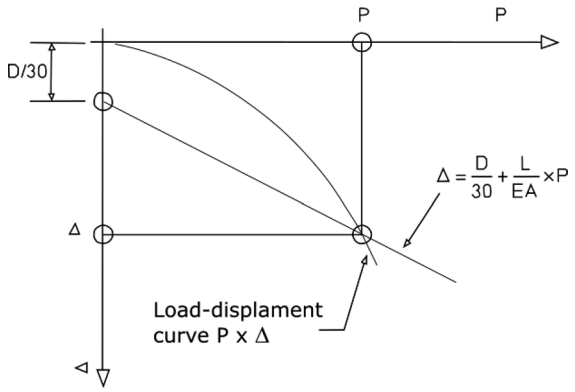

Fig. 14 Procedure provided by NBR 6122 to predict the bearing capacity of a pile from a load–displacement curve (adapted from ABNT 2019)

$$\Delta = \frac{D}{30} + \frac{L}{EA}P \tag{8}$$

where, Δ = settlement of the pile, D = shaft's diameter, L = length of the pile, E = Young's modulus of the pile, A = cross-sectional area of the pile, P = value of load used to plot the linear equation.

3 Results and Discussion

Initially, as it was previously described, the behavior of the single piles was simulated based on the t-z and q-z curves by Reese and O'Neill (1988), combined with the finite element method. The outcome of the simulation for the last load stage of the load test is presented in Fig. 15. Figure 15a shows the displacements along the pile, while Fig. 15b shows the load

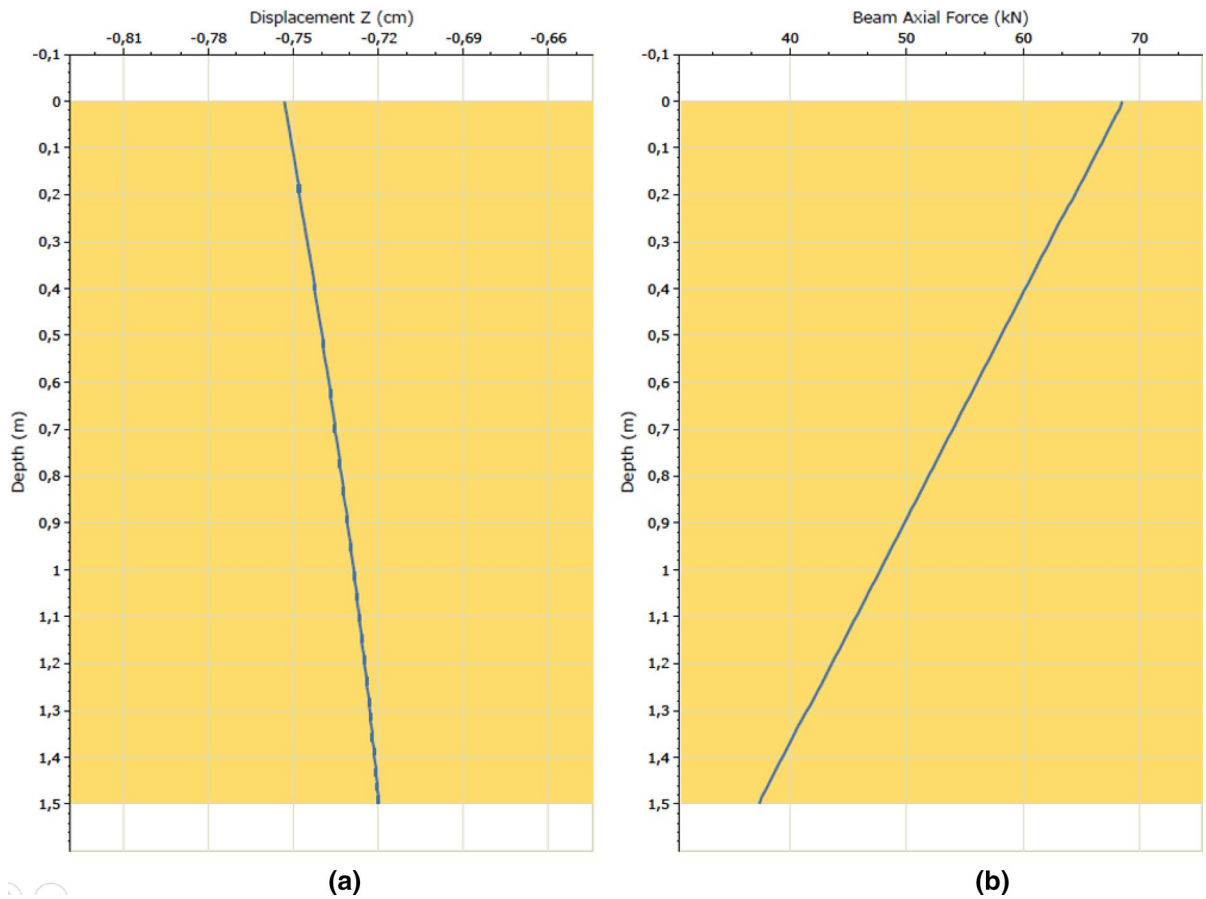

Fig. 15 Simulation of the (**a**) displacements along the pile and **b** load transfer diagram

transfer diagram. As commented, each load stage of the tests was simulated, and the displacements predicted for the top of the pile were used to generate the load–displacement curve of the single pile.

By the Fig. 15b, it can be observed a linear load transfer along the shaft. The maximum settlement was approximately 7.5 mm, on the top of the element, while the minimum was 7.2 mm at the pile's end. The difference between these two values, 0.3 mm, corresponds to the elastic shortening of the foundation. Figure 16 shows the model of the single pile simulated with the displacements indicated by a range of colors, it can be noted that the higher values of settlements are concentrated close to the top of the element.

Finally, Fig. 17 presents the load–displacement curve simulated for the single pile plotted along with both experimental curves for the caps with single piles. The vertical axis of the graphic presented in the mentioned figure gives the settlements (w), normalized by the shaft's diameter (D) of the piles, so the displacements can be read considering the size of the foundation. However, as all the piles have a 100 mm diameter and the values are expressed in percentage, the displacements of the vertical axis also represent the settlements in millimeters, as these values are numerically equal to the normalized data (w/D). The load tests for these caps were carried out with and without Styrofoam under the elements' ends in order to verify the distribution of load between shaft and tip.

By the load-displacements curves presented in Fig. 17, it is noted that the simulation predicted displacements very close to the experimental

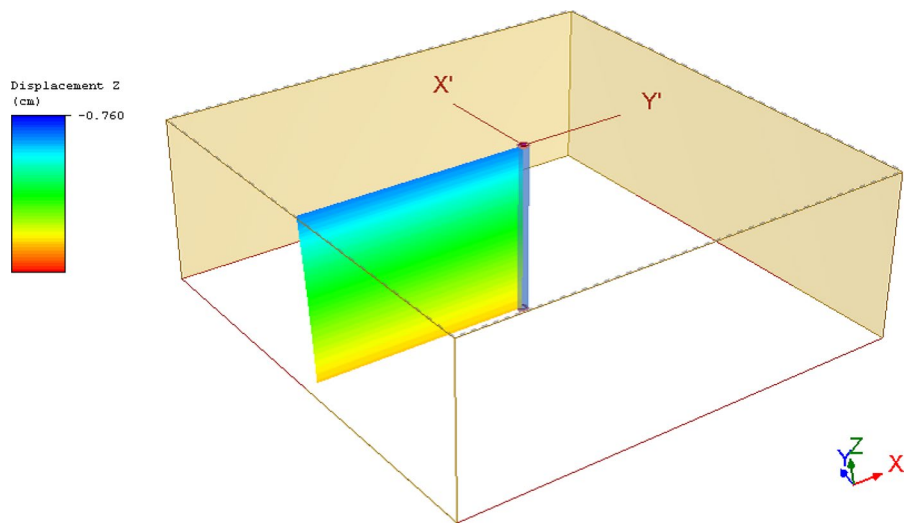

Fig. 16 Simulated model along with the predicted displacements

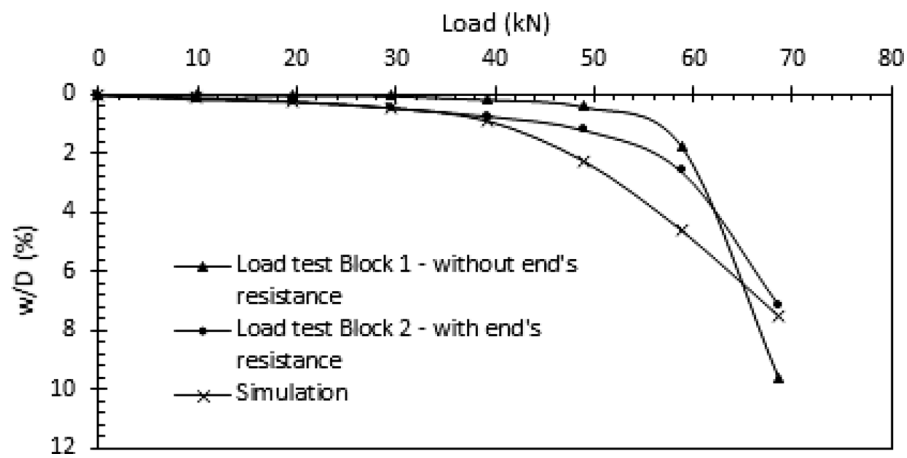

Fig. 17 Comparison between load–displacement curves simulated and experimental, for the single pile

values, especially until the load of 40 kN, which corresponds to elastic zone of the soil behavior. The working load of the piles (structural elements) is 50 kN, the allowable load of the soil-foundation system, as presented ahead, is 35 kN, therefore, the design load is 35 kN, for a safety factor equal to 2. Thus, the prediction shows agreement with the values recorded in the load tests for the design load.

Once simulated the load–displacement curve, the bearing capacity was determined by two different methods, Van der Veen (1953) and the one provided by the Brazilian technical rule NBR 6122 (ABNT 2019). The mentioned methods were also used to calculate the experimental bearing capacity, for this purpose it was used the curve of the cap 2, since both experimental curves were similar, leading to close values of bearing capacity. The bearing capacities determined from the curves presented in Fig. 8 are shown in Table 7.

Table 7 Bearing capacities of the single pile

Load–displacement curve	Method	
	NBR 6122	Van der Veen (1953)
Simulation (kN)	55	72
Experimental* (kN)	62	68.6

*cap 2—with end's resistance

The bearing capacity estimated by Van der Veen (1953) was 5% superior to the one determined from the experimental curve, showing excellent agreement between the values. The method of the NBR 6122 resulted in a bearing capacity 11% inferior to the experimental value. Thus, it can be observed that the predictions of bearing capacity made from the simulated curve, using both methods, showed good agreement with the values obtained through the load tests. It is worth mentioning that the highest percentual difference between the measured and predicted values of 11% represents an error in favor of safety.

The load–displacement curves of the pile groups were obtained from the single pile's curve combined with the settlement factors (ξ) calculated for each group, as it was previously described. Experimental values of the settlement factors (ξ), for the design load, of each group were calculated from the results of the load tests presented. The experimental values of the settlement factors (ξ) were plotted against the spacing for the groups of 2 and 4 piles, the graphic is shown in Fig. 18.

The 2 pile group with the relative spacing of 2 presented much higher displacements than the others, as it can be seen in Fig. 18. Apart from the mentioned group, it is observed a trend of increasing displacements with increasing spacing, such behavior is due to the greater bulbs of stress generated at the higher spacings, they mobilize larger portions of soil which causes an increase in the settlements.

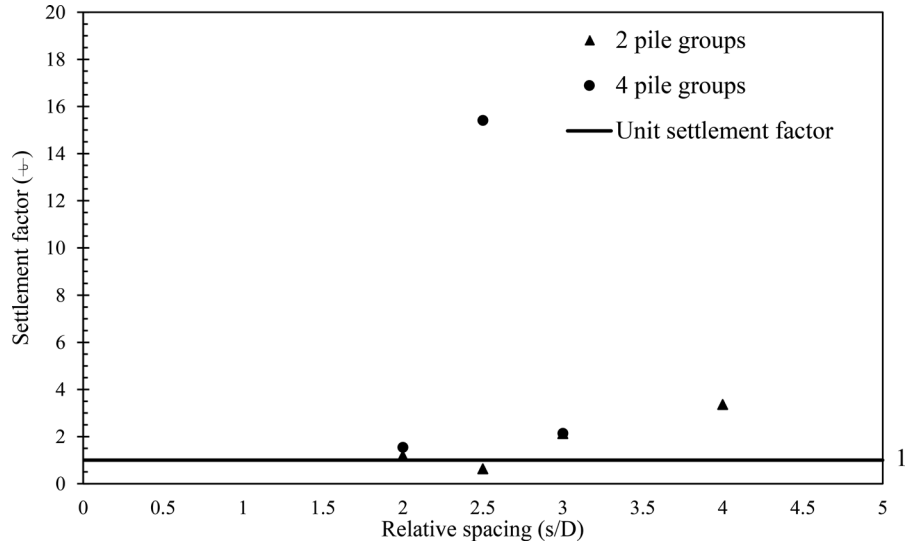

Fig. 18 Experimental settlement factors (x)

As previously explained, the method of Vesic (1969) was selected to estimate the settlement factors (ξ). The load–displacement curves of the pile groups were obtained by applying the settlement factor (ξ) of each group on the displacements of the single pile's curve and keeping the load per pile relation, as already described. In order to make the comparison viable, the simulated curves were compared to the experimental ones until the values of loads applied in the load tests. First, it was evaluated the settlement prediction of the simulations, then the bearing capacities obtained from the simulated curves were compared to the experimental values as well. One pile of the cap 10 presented failure during the load test, thus the comparisons couldn't be made for this case.

Figure 19 presents the comparison between the simulated and experimental load–displacement curves of the cap 3, composed of 2 piles with a 2 D spacing. The simulated curve shows excellent agreement with the experimental values along the entire curve. The settlement prediction is especially important for the design load, that is load under which the foundation may operate. For the 2 pile groups, the working load of the structural elements combined is 100 kN, while the allowable load for the cap 3 is 57 kN, for a safety factor of 2. The allowable loads for all the caps were determined by applying Van der Veen (1953) on the presented experimental load-displacements curves. Thus, in this case, the design load is 57 kN. Therefore, for the cap 3, the displacement prediction using the settlement factor (ξ) led to accurate results for the design load.

Figure 20 presents the comparison between the simulated and experimental load–displacement curves of the cap 4, composed of 2 piles with a 2.5 D spacing. The simulated curve shows good agreement with the experimental values until the load of 65 kN. In this case, the design load is 62 kN. Thus, the predictions were accurate until loads slightly superior than the reference value. Therefore, for the cap 4, the

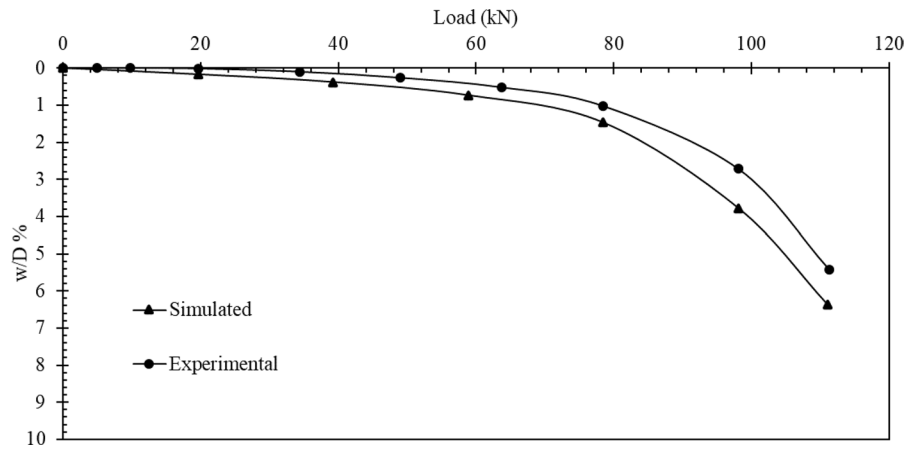

Fig. 19 Comparison between load–displacement curves simulated and experimental, for the cap 3, composed of 2 piles with a 2 D spacing

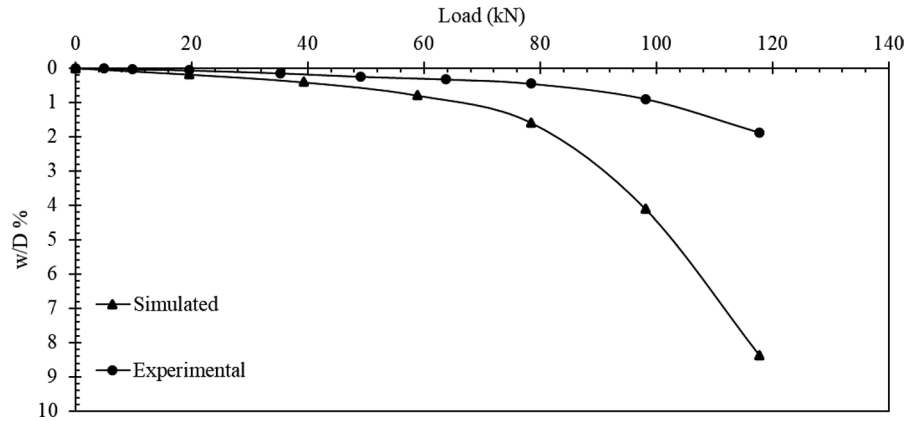

Fig. 20 Comparison between load–displacement curves simulated and experimental, for the cap 4, composed of 2 piles with a 2.5 D spacing

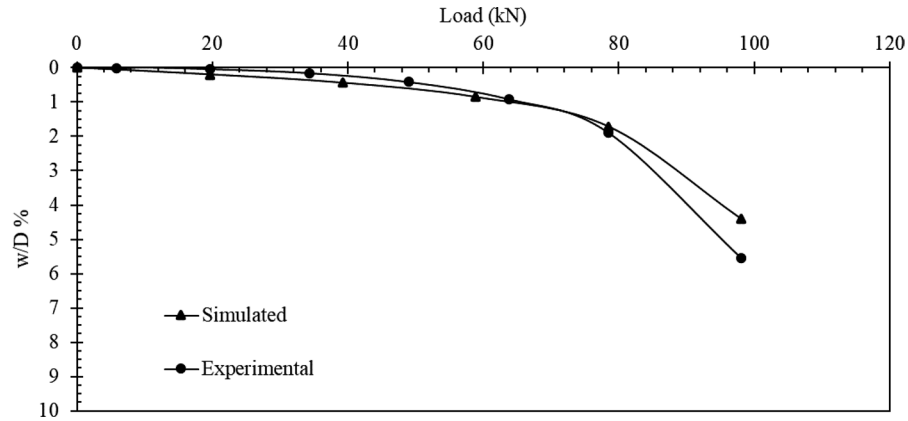

Fig. 21 Comparison between load–displacement curves simulated and experimental, for the cap 5, composed of 2 piles with a 3 D spacing

displacement prediction using the settlement factor (ξ) showed agreement for the design load.

Figure 21 presents the comparison between the simulated and experimental load–displacement curves of the cap 5, composed of 2 piles with a 3 D spacing. The simulated curve shows excellent agreement with the experimental values along the entire curve, but especially until the load of 80 kN. In this case, the design load is 50 kN. Thus, the predictions were accurate until loads 60% superior than the reference value. Therefore, for the cap 5, the displacement prediction using the settlement factor (ξ) showed agreement for the design load.

Figure 22 presents the comparison between the simulated and experimental load–displacement curves of the cap 6, composed of 2 piles with a 4 D spacing. The simulated curve shows excellent agreement with the experimental values until the load of 70 kN. In this case, the design load is 42 kN. Thus, the predictions were accurate until loads 67% superior than the reference value. Therefore, for the cap 6, the displacement prediction using the settlement factor (ξ) showed agreement for the design load.

Figure 23 presents the comparison between the simulated and experimental load–displacement curves of the cap 7, composed of 4 piles with a 2 D spacing. The simulated curve shows excellent agreement with the experimental values along the entire curve. For the 4 pile groups, the working load of the structural elements combined is 200 kN, while the allowable load for the cap 7 is 66 kN, for a safety factor of 2. Thus, in this case, the design load is 66 kN. Therefore, for the cap 7, the displacement prediction using the settlement factor (ξ) led to accurate results for the design load. It is worth to point out in this case of cap 7 the low level of the settlements.

Figure 24 presents the comparison between the simulated and experimental load–displacement curves of the cap 8, composed of 4 piles with a 2.5 D spacing. The simulated curve shows excellent

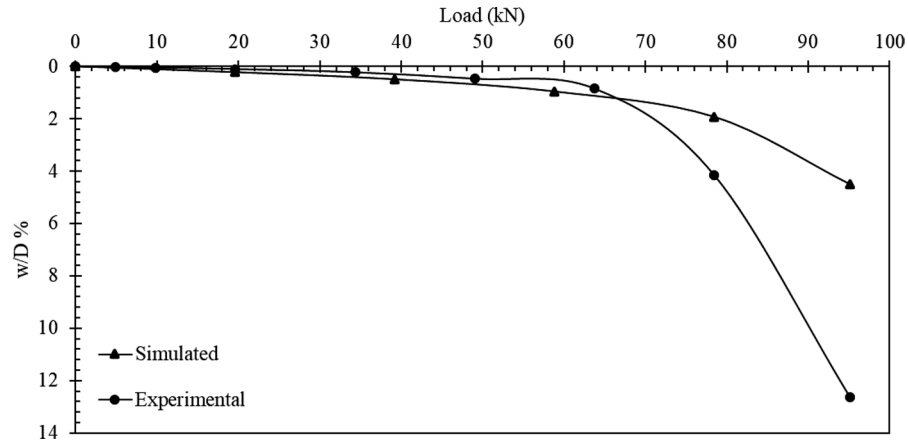

Fig. 22 Comparison between load–displacement curves simulated and experimental, for the cap 6, composed of 2 piles with a 4 D spacing

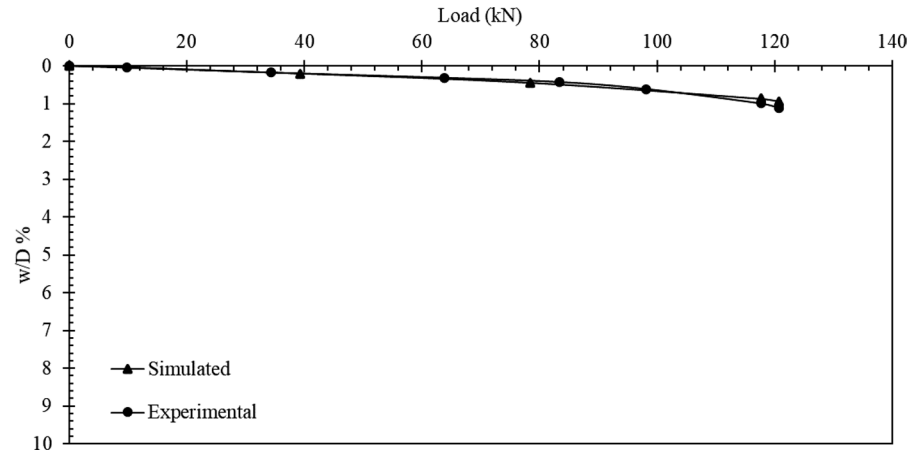

Fig. 23 Comparison between load–displacement curves simulated and experimental, for the cap 7, composed of 4 piles with a 2 D spacing

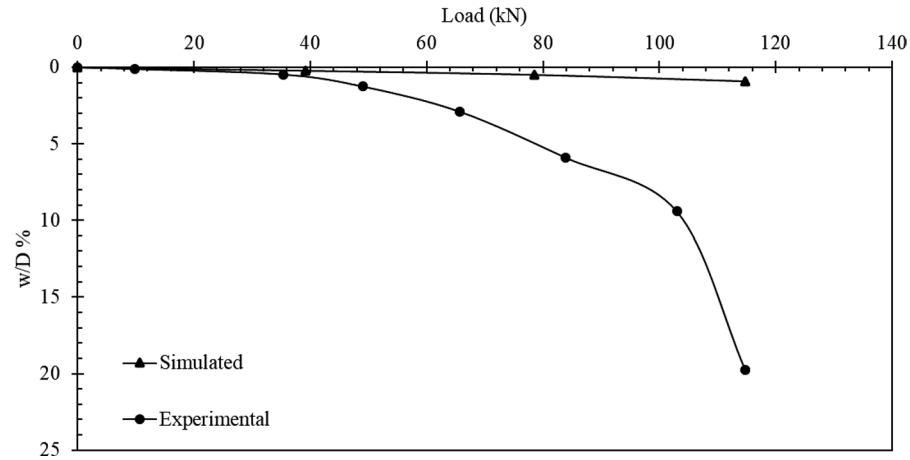

Fig. 24 Comparison between load–displacement curves simulated and experimental, for the cap 8, composed of 4 piles with a 2.5 D spacing

agreement with the experimental values until the load of 50 kN. In this case, the design load is 58 kN. Thus, the predictions were accurate until loads 14% inferior than the reference value. Therefore, for the cap 8, it was the only case in which the displacement prediction using the settlement factor (ξ) did not show agreement for the design load. It is worth to mention the high level recorded in the load tests for cap 8.

Figure 25 presents the comparison between the simulated and experimental load–displacement curves of the cap 9, composed of 4 piles with a 3 D spacing. The simulated curve shows excellent agreement with the experimental values until the load of 80 kN. In this case, the design load is 62 kN. Thus, the predictions were accurate until loads 30% superior than the reference value. Therefore, for the cap 9, the displacement prediction using the settlement factor (ξ) showed agreement for the design load.

Using the simulated load–displacement curves, the bearing capacities of the pile groups were estimated by two methods, Van der Veen (1953) and the one provided by the NBR 6122 (ABNT 2019). Table 8 presents a comparison of the values obtained through the simulated curves with the ones calculated from the results of the load tests.

Regarding the predictions made by Van der Veen (1953), it was possible to predict values for all the pile groups. The percentual difference between the simulated and experimental values for the caps 3 to 7 ranged from -1 to 5%, showing excellent agreement. The differences for the caps 8 and 9 was 20 and 14%, respectively. Thus, the methodology employed in this research was capable of predicting bearing capacities for pile groups accurately by using the method of Van der Veen (1953).

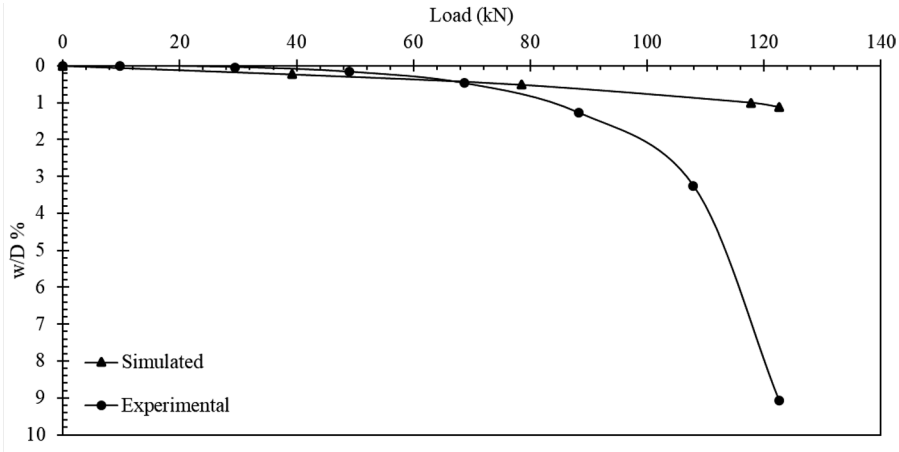

Fig. 25 Comparison between load–displacement curves simulated and experimental, for the cap 9, composed of 4 piles with a 3 D spacing

Table 8 Comparison between predicted and experimental values of the bearing capacities of the pile groups

Cap	n° piles/spacing	Van der Veen (1953)			NBR 6122		
		Simulated (kN)	Experimental (kN)	Difference (%)	Simulated (kN)	Experimental (kN)	Difference (%)
3	2/2	120	114	5	98	106	− 8
4	2/2.5	120	121.7	− 1	95	–	–
5	2/3	100	99	1	94	90	4
6	2/4	100	95.5	5	91	78	17
7	4/2	135	131.8	2	–	–	–
8	4/2.5	140	116.6	20	–	66	–
9	4/3	140	123.1	14	–	111	–

Due to the low level of settlements in some of the load–displacement curves, only the bearing capacities of the caps 3, 5 and 6 could be predicted by using the method provided by the NBR 6122 (ABNT 2019). For the mentioned caps the percentual difference between the simulated and experimental values calculated ranged from − 8 to 17%. Therefore, the usage of the method given by the brazilian technical rule wasn't effective in the case evaluated in this paper.

4 Conclusions

The concluding remarks of the present research are:

- The load–displacement curve obtained through the simulations based on load transfer functions combined with the finite element method was very similar to the experimental curves of the isolated piles, especially until the load of 40 kN, which is within the elasto-plastic zone of the soil's behavior. Therefore, the method employed was able to predict settlements accurately for the design load, which was of 35 kN for the isolated piles;
- The bearing capacities estimated from the simulated load–displacement curve of the single pile showed good agreement, for the both methods used of Van der Veen (1953) and the one provided by the NBR 6122 (ABNT, 2019), with the values determined from the curves obtained through the load tests. The error found in these predictions ranged from − 11% to 5%, this indicates that the methodology employed was effective in predicting bearing capacities;
- Regarding the simulations of the load–displacement curves of the pile groups using the settlement factor (ξ), the comparisons were made observing the agreement between simulated and

experimental load–displacement curves, giving special attention for the design loads. For caps 3, 5 and 7, predictions were accurate for the entire curves. For caps 6 and 9, predictions were accurate up to loads 67% and 30% superior to the design load, respectively. For cap 4, predictions were accurate up to loads slightly superior to the design load. Only for the cap 8, predictions were accurate up to loads 14% inferior than the design load. Thus, the usage of the t-z method combined with the settlement factor (ξ) to account for the pile group effect in the case evaluated in the present research was considered effective;

- Finally, the bearing capacities estimated by the method used in this study showed agreement with the data obtained through the load tests, when calculated by Van der Veen (1953). The percentual difference of the predicted values to the experimental ones ranged from -1 to 5% for the caps 3 to 7. The differences for the caps 8 and 9 was 20 and 14%, respectively. Therefore, as well as for the settlement prediction, the methodology employed in the present research was capable of estimating bearing capacities of pile groups accurately.

Acknowledgements To the Federal University of Ceará and Federal Institute of Ceará laboratorys for the cooperation in the tests performance, to the Post-graduate Program POSDEHA, to the Cearense Foundation for Scientific and Technological Development Support—FUNCAP and to the Coordination for the Improvement of Higher Education Personnel—CAPES for funding the research.

Data Availability The datasets analyzed during the current study are available in the institutional repository of the Federal University of Ceará, http://www.repositorio.ufc.br/handle/riufc/47920.

Code Availability RS Pile software was applied in this research.

Declarations

Conflict of interest The authors declare that they have no conflict of interest.

Consent for Publication The authors consent the manuscript may be published.

Consent to Participate Not applicable.

Ethics Approval Not applicable.

References

ABNT—Associação Brasileira de Normas Técnicas (2019) NBR 6122: design and construction of foundations. ABNT, Rio de Janeiro

Bonan VHF, Moura AS, Ayala GRL (2020) Experimental study of the group effect of short piles excavated in a granular soil profile. Ingeniare Rev Chil Ing. https://doi.org/10.4067/S0718-33052020000200323

Bonan VHF (2017) Estudo experimental do efeito de grupo de estacas escavadas em perfil de solo granular. Dissertation, Federal University of Ceara (UFC)

Cerqueira Junior E (2019) Avaliação da simulação do comportamento de grupo de estacas escavadas em perfil de solo granular a partir de funções de transferência de carga. Dissertation, Federal University of Ceara (UFC)

Cintra JCA, Aoki N (2010) Fundações por estacas: projeto geotécnico. São Paulo: Oficina de Textos. ISBN: 978–85–7975–004–5

Cunha RP, Poulos HG (2018) Importance of the excavation level on the prediction of the settlement pattern from piled raft analyses. Soils Rocks 41(1):91–99. https://doi.org/10.28927/sr.411091

Franke E, Muth G (1985) Scale effect in 1g model tests on horizontally loaded piles. In: Proceedings of the 11th international conference of soil mechanics and foundations, San Francisco, vol 2. pp 1011–1014

Garcia JR, Albuquerque PJR (2018) Influence of relative stiffness on the behavior of piled raft foundations. Acta Scientiarum Technol 40:e35209. https://doi.org/10.4025/actascitechnol.v40i1.35209

Mosher RL (1984) Load transfer criteria for numerical analysis of axially loaded piles in sand. U. S army waterways experiment station, automatic data processing center, Vicksburg, Mississippi

Moura AS, Ramos MR, Lima-Filho FP, Menezes PHLB, Cerqueira-Junior E (2018) Caracterização preliminar geotécnica do subsolo do Campo Experimental de Geotecnia e de Fundações da Universidade Federal do Ceará (CEGEF—UFC). In: Brazilian symposium of young geotechnical engineers—GeoJovem, Salvador

Nanda S, Patra NR (2014) Theoretical load-transfer curves along piles considering soil nonlinearity. J Geotech Geoenviron Eng 140(1):91–101. https://doi.org/10.1061/(asce)gt.1943-5606.0000997

Nasr AMA (2014) Experimental and theoretical studies of laterally loaded finned piles in sand. Can Geotech J 51:381–393. https://doi.org/10.1139/cgj-2013-0012

Reese LC, O'Neill MW (1988) Drilled shafts: construction procedures and design methods. Prepared for U.S. department of transportation, federal highway administration, in cooperation with the association of foundation drilling

Sharafkhah M, Sooshpasha I (2018) Physical modeling of behaviors of cast-in-place concrete piled raft compared to free-standing pile group in sand. J Rock Mech Geotech Eng 10(2018):703–716. https://doi.org/10.1016/j.jrmge.2017.12.007

Teixeira AH (1996) Projeto e execução de fundações. In: seminar of special foundation engineering and geotechnics, 3. São Paulo, Anais…São Paulo. vol 1. p 33–50

Van der Veen C (1953) The bearing capacity of a pile. In: International conference on soil mechanics and foundations engineering, 3. Zurich. vol 2. p 84–90

Velloso DA, Lopes FR (2010) Fundações: critérios de projeto, investigação do subsolo, fundações superficiais, fundações profundas. São Paulo: Oficina de Textos

Zhang J, Zhang S, Zhang Q, Liu S, Feng R (2018) Analysis of the response of an axially loaded pile considering softening behavior of pile-soil system. Soil Mech Found Eng. https://doi.org/10.1007/s11204-018-9497-1

Zhu H, Chang M (2002) Load transfer curves along bored piles considering modulus degradation. J Geotech Geoenviron Eng 128(9):764–774. https://doi.org/10.1061/(asce)1090-0241(2002)128:9(764)